

Noncontact tuning fork position sensing for hollow-pyramid near-field cantilevered probes

A. Ambrosio^{a)}

Dipartimento di Fisica "Enrico Fermi," Università di Pisa, Largo Bruno Pontecorvo 3, 56127 Pisa, Italy

E. Cefali, S. Spadaro, and S. Patanè^{b)}

Dipartimento di Fisica della Materia e Tecnologie Fisiche Avanzate, Università di Messina, Salita Sperone 31, 98166 Messina, Italy

M. Allegrini^{c)}

Physics Laboratory, National Institute of Science and Technology, Gaithersburg, Maryland 20899

D. Albert

Institute of Technical Physics, University of Kassel, 34109 Kassel, Germany

E. Oesterschulze

Physik und Technologie der Nanostrukturen, Technische Universität Kaiserslautern, Erwin-Schrödinger-Straße, 67663 Kaiserslautern, Germany

(Received 29 June 2006; accepted 29 August 2006; published online 17 October 2006)

We demonstrate that tuning fork sensing provides a stable, noncontact mode of operation when applied to near-field optical microscopy employing cantilevered probes. Detrimental damping effects that have so far limited the practical use of these otherwise very advantageous probes are totally overcome. We validate our tuning fork setup featuring hollow-pyramid probes by an optical nanolithography application. © 2006 American Institute of Physics.

[DOI: [10.1063/1.2362588](https://doi.org/10.1063/1.2362588)]

Surface optical imaging with nanometric spatial resolution is commonly attained by scanning near-field optical microscopy (SNOM).^{1,2} The so-called aperture SNOM works by scanning a small aperture in close proximity to the sample surface. Typical SNOM aperture probes are optical fibers, tapered and metal coated at the apex. The SNOM resolution is given by the size of their apical aperture, typically in the 20–100 nm range. Fabrication is usually accomplished either by heat-and-pull^{3,4} or by chemical etching methods.^{5–7} A variety of reliable tapered SNOM probes is commercially available, but their performances are intrinsically limited by the low power throughput (10^{-3} in the best cases^{8,9}). They also suffer thermal effects^{10–13} due to partial energy absorption by the metallic coating, and polarization selection/control is difficult.^{14,15} Hollow-pyramid cantilevered^{16,17} (HPC) probes seem to solve all the above mentioned problems encountered with tapered optical fibers. HPC feature small apertures (size of 40–150 nm depends on process conditions during fabrication) together with a large taper angle of 70.5° ensuing high optical throughput.^{18,19} It is remarkable that the pyramidal geometry does not affect the duration of short laser pulses²⁰ while preserving a well defined polarization state.^{17,21} Silicon dioxide as tip material guarantees excellent mechanical stability for long life performance. Their integration in a conventional SNOM setup is straightforward. Because of their cantilever geometry known from atomic force microscopy (AFM) probes, the stabilization of the tip-sample distance can be accomplished by techniques directly

imported by the AFM world. Contact mode operation of these probes while simultaneously monitoring the near-field optical transmission signal is quite simple to implement also in commercial setups. Nevertheless, lifetime of the tip is an important issue and therefore it is desirable to prevent the aperture from damage by operating the probe in the noncontact or tapping mode. In this case one has to put up with well known effects such as the slow transient response of the cantilever and the instabilities due to the high quality factor.²² Moreover, the shape of the cantilever leads to damping effects produced by the thin air cushion between the cantilever and the surface.²³ This problem has been partially overcome by increasing the angle between the sample surface and the cantilever or by more intricate methods, such as drilling a number of microholes in the cantilever body to permit air to escape.^{23,24}

Here, we demonstrate how to use hollow cantilevered tips in scanning near-field optical microscopy while avoiding detrimental damping effects that are normally present in both the contact mode of operation and also in the tapping mode. Tip lifetime is hence well preserved. The method simply consists in using the shear force to detect and control the tip to sample distance. The sensor used to detect the shear force amplitude is a tuning fork; therefore the electrical signals are easily managed by the electronic circuit of a standard SNOM without any modification. Since it was introduced,²⁵ this method has been largely used in SNOM setup. We have simply adapted it to HPC tips that are mounted on the tuning fork setup to fit the head of an existing homemade SNOM.²⁶ The performance of this setup is validated by a nanolithography experiment at 404 nm on an azopolymethacrylate (PMA4) thin film.

The HPC is installed in an existing setup based on a commercially available microscope (Zeiss Axiovert). The

^{a)}Present address: CNR-INFM CRS COHERENTIA and Dipartimento di Scienze Fisiche, Università di Napoli "Federico II," Via Cintia, I-80126 Napoli, Italy; electronic mail: tony@na.infn.it

^{b)}Electronic mail: patanes@unime.it

^{c)}On sabbatical leave from Dipartimento di Fisica "Enrico Fermi," Università di Pisa, Largo Bruno Pontecorvo 3, I-56127 Pisa, Italy.

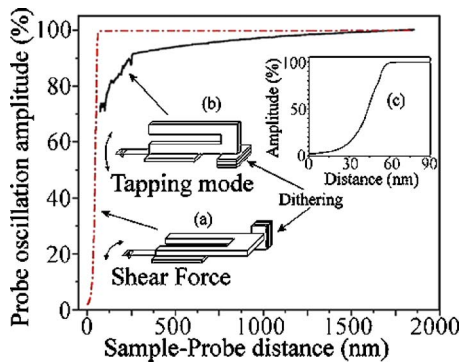


FIG. 1. (Color online) Approaching curves in shear force (dashed dotted curve) and tapping mode (continuous line). Inserts (a) and (b) show sketches of the HPC installed on the tuning fork in the shear force mode and in the tapping mode configuration, respectively. Insert (c) shows a blow up of the shear force approaching curve for short distances.

shear force working mode is obtained by gluing the entire chip carrying the HPC tip onto the wide side of one arm of a common quartz tuning fork. The fundamental mode of the tuning fork at 32 kHz produces the mechanical oscillation of the cantilever, as required by the shear force configuration. An xyz -translational stage holds the tuning fork system. This stage is used to bring the HPC hole to the focus of the microscope objective in order to couple the laser source to the probe. Light coupling is favored by a low numerical aperture (NA) optical objective and we use a $10\times 0,2$ NA Epiplan Zeiss objective. A four quadrant piezotube holds and moves the sample that is installed beside the shear force assembly. The light signal, in transmission mode, is collected by a PCX lens lodged inside the tube with a Hamamatsu miniaturized phototube.

As a proof of principle, we show in Fig. 1 one approaching curve (solid line) recorded in tapping mode [in the geometry shown in the insert (b) of Fig. 1] together with the approaching curve (dashed-dotted line) obtained with the same cantilever (nominal aperture 100 nm) mounted on the tuning fork in the shear force geometry [shown in the insert (a) of Fig. 1]. The tapping mode curve clearly shows a damping effect due to the air layer between the sample surface and the cantilever body. This damping is present also at a distance quite far from the working point and it may lead to a false approach or, in the worst case, to loss of the feedback control. In addition, the tapping mode requires a linearization procedure to control the tip-sample distance because of the nonlinear trend²⁷ of the tip-sample interaction. The shear force configuration overcomes these two difficulties in a single step. In this case, the amplitude of the oscillations has an almost linear dependence on the probe-sample distance²⁸ and the damping effect due to the air layer disappears because the horizontal motion of the HPC does not create any pressure gradient. The shear force approaching curve we report in Fig. 1 shows indeed no air damping. The expected linear dependence from the distance is clearly seen in the blowup of insert (c) from 100% down to 25% of the free oscillation amplitude. For distances shorter than 30 nm the linearity is lost because of tip dimension effects and force perturbations caused by humidity, capillarity, electrostatic interactions, etc.²⁹

To test the topographic performance of the method, the surface of an AFM commercial test pattern (Veeco InstrumentsTM) was imaged over an $8\times 8\ \mu\text{m}^2$ area and the result

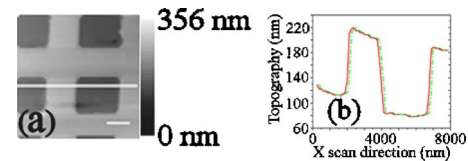


FIG. 2. (Color online) (a) Topographic image acquired on an AFM test pattern (VeecoTM). Scan area of $8\times 8\ \mu\text{m}^2$. Scale bar of 1.5 μm . (b) Profile line extracted on the forward (solid line) and backward (dot-dashed line) scans along the line marked on the image (a).

is shown in Fig. 2(a). The line profiles in the forward and backward scanning directions [Fig. 2(b)] along the line indicated on the image are almost identical, proving that the system gives very good topographic stabilization suitable for use in SNOM. This was additionally verified by imaging a $3\times 2.2\ \mu\text{m}^2$ wide surface of an aluminum pattern deposited on a glass cover slip. The optical image [Fig. 3(b)] was acquired in transmission mode using a solid state laser source at 635 nm. As expected, the metallic islands are observed as a small relief in the topographic image [Fig. 3(a)] and dark zones in the optical image [Fig. 3(b)]. The edge optical resolution is about 80 nm with a contrast of about 35%. These results are compatible with the hole size of the near-field sensor used for this test, which has a nominal aperture of 120 nm.

To validate the performance of our tuning fork setup using HPC probes, we report a practical application, namely, near-field optical nanolithography. The experiment consists in exciting *trans-cis-trans*-isomerization cycles on a 100 nm thick film of azobenzene side-chain polymethacrylate polymer (PMA/PMA4).³⁰ With a SNOM working with ordinary tapered fiber probes, we have already demonstrated via topography³¹ as well as via optical birefringence³² that these azobased polymers are appropriate for near-field optical nanowriting. Thus, it is straightforward to compare the near-field nanolithography obtained with hollow cantilevered probes with previous results. This test gives a precise measure of the light throughput of the HPC sensors and of the long term mechanical stability of the instrument, confirming the excellent topographic and optical performances. The optical absorption spectrum of PMA4 spin-coated thin films ranges from 360 to 440 nm. In this range, complete *trans-cis-trans*-isomerization of the azobenzene group takes place^{33,34} and induces motion of molecules leading to a deformation of the polymeric matrix. We use a 4 mW solid state laser emitting at 404 nm. Figure 4(a) shows the topographical image of an area of the sample surface, acquired with the laser off. As a check of the instrument's long term stability, a series of dots each with an exposure time ranging from 15 to 30 s was written and then imaged by scanning the surface again with the HPC probe, as shown in Figs. 4(b)–4(d). The height of the dots, the input laser power, and the exposure time provide a value of 6×10^{-3} for the throughput of the cantilevered probe. That means that near-

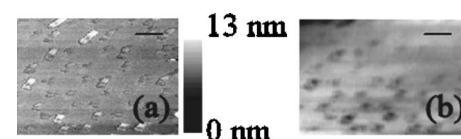


FIG. 3. Topographic (a) and optical (b) images collected in transmission mode of an Al pattern deposited on a glass cover slip. Scale bar=500 nm.

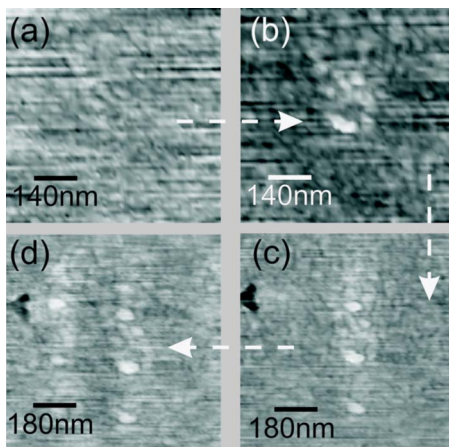


FIG. 4. (Color online) Four frames showing the consecutive writing of five dots (protrusions) on the free surface of a PMA/PMA4 copolymer film. (a) SNOM topographical image of the area before writing. (b) Image of the first dot drawn. (c) Two dots added to the first one. (d) Result of the complete process. These dots are not taller than 14 nm due to the short exposure time of 15–30 s for each dot.

field optical nanolithography can be achieved with only ~ 12 nW of laser power. By observing the height and the shape of the structures obtained with an exposure time of about 15 s, it appears that the dots in Fig. 4 are not completely formed. They have an average height of about 10 nm with a full width at half maximum not larger than 50 nm. This is in good agreement with the polymeric film properties and means that the HPC sensor working in shear force mode is able to image topographic structures below 10 nm. The complete process (writing, imaging, and writing again), shown in Fig. 4, took several hours. As it is evident from the images, in this time interval, no drifts have occurred confirming the high degree of stabilization we have achieved in our setup.

In conclusion, we demonstrate that hollow-pyramid cantilevered near-field probes readily work in the shear force mode. The tuning fork setup requires little modification of a standard near-field optical microscope. The method is not susceptible to damping effects from the air layer between the sample and the probe providing superior control of the sample to probe distance. The shear force mode of operation avoids contact with the sample surface; hence it considerably extends the HPC probe tip life span. The rugged setup based on a standard optical microscope guarantees stability even over long duration measurement runs. This simple, all-piezoelectric sensing method using HPC near-field probes is expected to open the way to several near-field applications. As a performance test and example, we have here reported near-field optical lithography on azopolymeric films by means of cantilevered hollow probes.

The authors gratefully acknowledge many helpful discussions with Francesco Fusco. Certain commercial equipment, instruments, or materials are identified in this work to

specify the experimental procedure adequately. Such identification is not intended to imply recommendation or endorsement by the National Institute of Standards and Technology, nor it is intended to imply that the materials or equipment identified are necessarily the best available for this purpose.

- ¹D. W. Pohl, W. Denk, and M. Lanz, *Appl. Phys. Lett.* **44**, 651 (1984).
- ²A. Lewis, M. Isaacson, A. Harootunian, and A. Murray, *Ultramicroscopy* **13**, 227 (1984).
- ³E. Betzig, J. K. Trautman, T. D. Harris, J. S. Weiner, and R. L. Kostelak, *Science* **251**, 1468 (1991).
- ⁴G. A. Valaskovic, M. Holton, and G. H. Morrison, *Appl. Opt.* **34**, 1215 (1995).
- ⁵D. R. Turner, U.S. Patent No. 4,469,554 (4 May 1983).
- ⁶P. Lambelet, A. Sayah, M. Pfeffer, C. Philipona, and F. Marquis-Weible, *Appl. Opt.* **37**, 7289 (1998).
- ⁷R. Stöckle, C. Fokas, V. Deckert, R. Zenobi, B. Sick, B. Hecht, and U. P. Wild, *Appl. Phys. Lett.* **75**, 160 (1999).
- ⁸D. Zeisel, S. Nettesheim, B. Dutoit, and R. Zenobi, *Appl. Phys. Lett.* **68**, 2491 (1996).
- ⁹T. Held, S. Emonin, O. Marti, and O. Hollricher, *Rev. Sci. Instrum.* **71**, 3118 (2000).
- ¹⁰M. Stähelin, M. A. Bopp, G. Tarrach, A. J. Meixner, and I. Zschokke-Gränacher, *Appl. Phys. Lett.* **68**, 2603 (1996).
- ¹¹Ch. Lienau, A. Richter, and T. Elsaesser, *Appl. Phys. Lett.* **69**, 325 (1996).
- ¹²P. G. Gucciardi, M. Colocci, M. Labardi, and M. Allegrini, *Appl. Phys. Lett.* **75**, 3408 (1999).
- ¹³A. Ambrosio, O. Fenwick, F. Cacialli, R. Micheletto, Y. Kawakami, P. G. Gucciardi, D. J. Kang, and M. Allegrini, *J. Appl. Phys.* **99**, 084303 (2006).
- ¹⁴V. Sandoghdar and J. Mlynek, *J. Opt. A, Pure Appl. Opt.* **1**, 523 (1999).
- ¹⁵L. Ramoino, M. Labardi, N. Maghelli, N. Maghelli, L. Pardi, M. Allegrini, and S. Patanè, *Rev. Sci. Instrum.* **73**, 2051 (2002).
- ¹⁶C. Mihalcea, W. Scholz, S. Werner, S. Münster, E. Oesterschulze, and R. Kassing, *Appl. Phys. Lett.* **68**, 3531 (1996).
- ¹⁷E. Oesterschulze, O. Rudow, C. Mihalcea, W. Scholz, and S. Werner, *Ultramicroscopy* **71**, 85 (1998).
- ¹⁸A. Vollkopf, O. Rudow, and E. Oesterschulze, *J. Electrochem. Soc.* **148**, G587 (2001).
- ¹⁹G. Georgiev, M. Müller-Wiegand, A. Georgieva, K. Ludolph, and E. Oesterschulze, *J. Vac. Sci. Technol. B* **21**, 1361 (2003).
- ²⁰M. Labardi, M. Zavelani-Rossi, D. Polli, G. Cerullo, M. Allegrini, S. De Silvestri, and O. Svelto, *Appl. Phys. Lett.* **86**, 031105 (2005).
- ²¹P. Biagioni, D. Polli, M. Labardi, A. Pucci, G. Ruggeri, G. Cerullo, M. Finazzi, and L. Duò, *Appl. Phys. Lett.* **87**, 223112 (2005); *Appl. Phys. Lett.* **88**, 209901(E) (2006).
- ²²T. Kowalewski and J. Legleiter, *J. Appl. Phys.* **99**, 064903 (2006).
- ²³P. N. Minh, T. Ono, and M. Esashi, *Sens. Actuators, A* **80**, 163 (2000).
- ²⁴P. N. Minh, T. Ono, and M. Esashi, *Rev. Sci. Instrum.* **71**, 3111 (2000).
- ²⁵K. Karrai and R. D. Grober, *Appl. Phys. Lett.* **66**, 1842 (1995).
- ²⁶E. Cefali, S. Patanè, P. G. Gucciardi, M. Labardi, and M. Allegrini, *J. Microsc.* **210**, 262 (2003).
- ²⁷R. Garcia and R. Pérez, *Surf. Sci. Rep.* **47**, 197 (2002).
- ²⁸C. Durkan and I. V. Shvets, *J. Appl. Phys.* **80**, 5661 (1996).
- ²⁹K. Karrai and I. Tieman, *Phys. Rev. B* **62**, 13174 (2000).
- ³⁰A. S. Angeloni, D. Caretti, M. Laus, E. Chiellini, and G. Galli, *J. Polym. Sci. [A1]* **29**, 1865 (1995).
- ³¹S. Patanè, A. Arena, M. Allegrini, L. Andreozzi, M. Faetti, and M. Giordano, *Opt. Commun.* **210**, 37 (2002).
- ³²V. Likodimos, M. Labardi, L. Pardi, M. Allegrini, M. Giordano, A. Arena, and S. Patanè, *Appl. Phys. Lett.* **82**, 3313 (2003).
- ³³S. Havilsted, F. Andruzzi, C. Kulinna, H. W. Siesler, and P. S. Ramanujam, *Macromolecules* **28**, 2172 (1995).
- ³⁴K. Ichimura, S. Morino, and H. Akiyama, *Appl. Phys. Lett.* **73**, 921 (1998).